ELSEVIER

Journal of Molecular Catalysis A: Chemical 166 (2001) 87–99

JOURNAL OF MOLECULAR CATALYSIS A: CHEMICAL

www.elsevier.com/locate/molcata

Acid and redox properties of Co-substituted aluminium phosphates

F. Corà [a,*], C.R.A. Catlow [a], A. D'Ercole [b]

[a] *Davy-Faraday Research Laboratory, The Royal Institution of Great Britain, 21 Albemarle Street, London W1X 4BS, UK*
[b] *Theoretical Chemistry Group, University of Torino, Via Giuria 5, I-10125 Torino, Italy*

Abstract

Ab initio quantum chemical techniques are applied to the investigation of structural and bonding properties of microporous aluminophosphates and gallophosphates. The calculations find a close measure of agreement with experimental structural data. The bonding in the materials is shown to be of 'molecular-ionic' character, i.e. comprising Al^{3+} (Ga^{3+}) and PO_4^{3-} ions. Calculated redox energies are reported for Co-substituted materials.

Keywords: Redox properties; Zeolites; Aluminium phosphates; Gallium phosphate

1. Introduction

Microporous silicates, or zeolites, have been intensively investigated in recent years for their applications in gas separation, ion exchange and heterogeneous catalysis, all processes that exploit the geometric selectivity allowed by the porous framework architecture towards the diffusion of molecular species through the structure [1]. The economic importance of these processes, especially in the synthetic chemistry industry, which relies on the availability of new and improved catalysts, has led to continuous attempts to extend the range of microporous compounds available [2]. The class of microporous crystalline materials synthesized includes now a rich variety of structures, and with different composition, from the SiO_2-based zeolites to aluminium and gallium phosphates (AlPO's and GaPO's), pure or with heteroatom substitutions, to the octahedral molecular sieves (OMS) based on MnO_2 [3–5]. Our recent attempt to design microporous structures of early transition metal oxides, such as MoO_3 and WO_3 [6,7], also goes in this direction.

In the present paper, we limit our attention to zeotypic materials, whose framework is based on corner-sharing of tetrahedral (TO_4) building units, and contrast the general properties of SiO_2, AlPO and GaPO compounds via accurate quantum-mechanical (QM) calculations.

In the pure SiO_2 form, or when Si is replaced by stoichiometric amounts of +3 and +5 ions such as Al and P, the zeolitic framework is chemically inert. If, however, a charge imbalance occurs in the framework, for instance, by replacing a Si^{4+} cation with Al^{3+}, the framework is chemically activated. The overall negative charge of the tetrahedral backbone is compensated by extraframework cations or by acid protons; in the latter case, the resulting Brønsted acidity of Al-doped zeolites is used in a range of acid-activated heterogeneous catalytic reactions. Framework Si atoms may also be replaced by transition metal cations, such as Ti^{4+}, which confer *redox* capability on the solid catalyst [8,9].

As a general rule, only heteroatoms with the same charge, or at most a difference of −1, from the charge of the host cation, can be inserted as isolated substitutional dopants in zeotypic frameworks. The range of heteroatom substitutions that can be achieved in SiO_2

* Corresponding author.
E-mail address: furio@ri.ac.uk (F. Corà).

1381-1169/01/$ – see front matter
PII: S1381-1169(00)00469-6

zeolites is, therefore, limited to 3+ and 4+ cations; the different partition of positive charge between the T-sites in AlPO and GaPO molecular sieves allows instead a much more extensive range of dopants, whose formal charge can vary from +2 to +5. Late transition metal ions, such as $Mn^{II/III}$, $Co^{II/III}$ or $Fe^{II/III}$ can be readily incorporated in AlPO's [10,11] (to form the so-called Me-AlPO compounds), but not in zeolites. The ease of these transition metal ions, when substituted for Al in the AlPO framework, to undergo both redox and acid/base reactions confers on Me-AlPO's a greater flexibility towards heterogeneous catalysis, than is available in zeolites. For instance, Co-AlPO and Mn-AlPO catalysts have recently been shown to oxidise linear alkanes using molecular oxygen as reagent, rather than more expensive sacrificial oxidants such as organic hydroperoxides [12,13].

Several problems remain open from the experimental work, related to the local structure and redox properties of the active sites in Me-AlPO's; for instance, only a fraction of the substitutional Co ions in Co-AlPO's (those that can be reoxidised to oxidation state +3 upon calcination) appear to be catalytically active. Moreover, EXAFS studies suggest a coordination number lower than 4 for the framework Co^{III} ions, inconsistent with the simple replacement of a framework Al^{3+} ion by Co^{3+} [14]. The instability of the microporous AlPO framework towards denser phases upon high loadings of transition metal ions is another unsolved problem. Insight from theoretical work may substantially contribute to answering the above questions, and hence to progress towards the synthesis of improved Me-AlPO catalysts.

Little information exists currently in the theoretical chemistry literature relating to the atomic-level details of AlPO's and Me-AlPO's materials, which is due to the requirements that computational methods should satisfy for being realistically applied to microporous aluminium and/or gallium phosphates.

Early QM theoretical studies to investigate the structure and reactivity of heteroatoms in zeolites, have been performed via isolated cluster models, in which a small molecular fragment is cut from the crystalline SiO_2 framework, and is assumed to represent the solid catalyst in the close neighbourhood of the active site (see, e.g. [15]). On the assumption that the SiO_2 framework is composed of a continuous backbone of Si–O covalent bonds, the Si–O bonds cleaved on forming the cluster are saturated with H atoms; this saturation avoids the presence of spurious dangling bonds in the description of the fragment.

QM studies using small molecular fragments can provide very accurate information on the electronic structure and energetics of chemical reactions occurring at the active sites, and cluster models, either isolated [16,17] or with more or less sophisticated forms of embedding potentials (see [18,19]), are still a widely exploited tool to investigate the reactivity of zeolites.

The extension of cluster studies to model AlPO and GaPO frameworks, however, is not as straightforward as could be imagined by their structural analogy with zeolites. The problem is linked to the different charge of the framework Al (Ga) and P ions; in Fig. 1 we compare the properties of a 2-T sites cluster representing SiO_2 and AlPO materials. If not accurately selected, molecular fragments cut out of an AlPO framework, are either charged, or affected by an intense Coulomb field gradient across the structure. Neither situation provides an accurate description of the crystalline environment in which the Al and P ions are hosted; in the real materials, the long-range ordered alternance of Al and P ions balances their different charges, and gives rise to a smooth Madelung field in the interstitial regions. The above limitation may severely affect the reliability of cluster-model calculations to simulate chemical reactions occurring in AlPO's, and cluster models appear generally inadequate to represent the AlPO framework.

An alternative description of AlPO's, and of the effect of heteroatom substitutions, can be obtained by describing the framework under periodic boundary conditions. A correct description of the crystalline environment and of the Madelung field can thus be achieved, which, however, requires a more expensive theoretical treatment, which has to employ the same degree of accuracy both for the active site and for the rest of the solid. Most microporous AlPO's have large unit cells, and low symmetry, making periodic studies computationally very demanding. It is only with the most recent developments of both hardware and software that such calculations have become feasible; this fact largely explains the lack of theoretical data on AlPO's in the present literature.

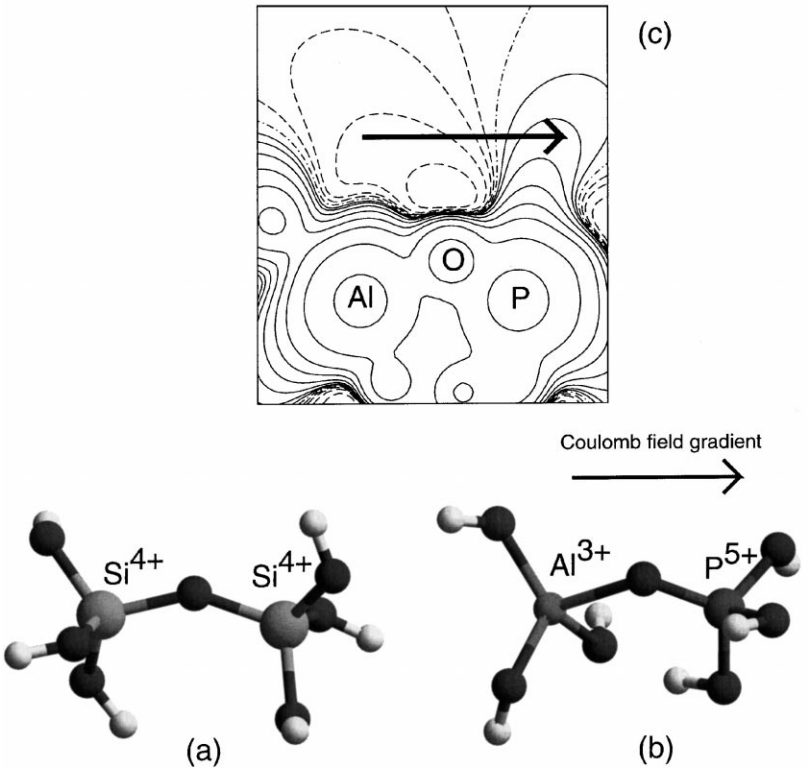

Fig. 1. Structure of 2-T sites clusters representing microporous frameworks of composition SiO_2 (a) and AlPO (b). Electrostatic potential generated by the AlPO fragment (c); continuous, dashed and dot-dashed lines correspond to positive, negative and zero values of the potential. The geometry of the clusters has been completely optimised using DMOL^3 and the same computational parameters employed in the periodic calculations; in the AlPO fragment (b), the direction of the terminal OH groups is bent by the strong Coulomb field, and all the H atoms point towards the Al position.

The periodic QM calculations that we have performed, and shall report in the present paper, are a first attempt to fill this gap of information. Results are divided in two sections: in the first, we deal with the undoped AlPO and GaPO framework to provide a general assessment of the techniques employed and of the properties of the host system; in the second, we examine the Co/Al substitution in AlPO-34, and hence a set of problems closer to the catalytic applications of the materials examined.

2. Computational details

We have employed two different computer codes, namely CRYSTAL [20,21] and DMOL^3 [22,23], to investigate crystalline AlPO and GaPO materials. Both codes are based on periodic boundary conditions, and describe the electronic distribution of the systems with a linear combination of atomic orbitals; all the other methodological details are, however, different:

- The basis set in CRYSTAL is expressed analytically as a contraction of Gaussian-type orbitals, while DMOL^3 employs a numerical definition of the basis functions in a grid of points surrounding the atom to which they are associated.
- The truncation of integrals, necessary to describe the Coulomb and exchange interactions in infinite systems, is achieved in DMOL^3 by limiting the spatial extent of the basis functions (5.5 Å in our case); in CRYSTAL by selecting a series of overlap ‘cut-offs’ (we used the default values of 6, 6,

6, 6, 12), beyond which integrals are disregarded or evaluated by Ewald summations.

- Although CRYSTAL allows the use of both Hartree–Fock (HF) and density functional (DF) Hamiltonians, we have performed only HF studies with the code; DF calculations, using the gradient-corrected functional of Perdew and Wang [24], have instead been performed with DMOL^3.
- A further difference between the two methods relates to the sampling of reciprocal space, necessary to represent the dispersion of energy levels: a regular array of $3 \times 3 \times 3k$-points has been employed in CRYSTAL for the calculations on Berlinite (quartz) structured AlPO and GaPO frameworks, reduced to $2 \times 2 \times 2$ for the microporous materials with larger unit cells; calculations with DMOL^3 are instead limited to a single k-point. Given the large band-gap and the relatively large unit cells of the materials examined, however, a single k-point is sufficient to provide accurate results.
- Finally, geometry optimisations have been performed numerically with CRYSTAL, optimising both cell parameters and internal coordinates, and analytically with DMOL^3, limiting the parameters optimised to the internal coordinates. In both cases, the geometry optimisation has been stopped at a convergence of 10^{-5} Ha in the internal energy.

Consistency of the results obtained with the two codes, given the complementary methodological choices outlined above, is a good indirect test for the performance of both in the problem examined.

The effect of different basis sets on the modelling of zeolites has been extensively examined with CRYSTAL in [25]. Such a methodological study is not repeated here for AlPO's and GaPO's; we shall instead assume that the findings of [25] are transferable from zeolites to AlPO's and GaPO's. In both CRYSTAL and DMOL^3 calculations, we used a basis set of split-valence plus polarisation quality for each atom of the structure. The performance of such a combination of basis functions was shown to be satisfactory in [25]. In DMOL^3 we used the standard DNP basis set, while in CRYSTAL we derived the basis set from previous publications [25–27], and reoptimised the outer-valence sp and the polarisation d exponents in the berlinite phase. Details of the basis set optimisation will be given in a future publication, and are available from the authors upon request.

The strategy that we have adopted in the study is the following: first, we have examined, using CRYSTAL, four different polymorphs of pure AlPO and GaPO composition isostructural to the α-quartz (QUA), sodalite (SOD), chabazite (CHA) and ATN polymorphs of silica. In the following sections, we employ the labels QUA, SOD, CHA and ATN to refer to the four structures. We then compared the result for AlPO-34 (CHA) obtained with CRYSTAL and DMOL^3; finally, we have employed the latter to examine the doping of AlPO-34 with Co.

3. The host AlPO and GaPO frameworks

In the first step of our calculations, performed with the CRYSTAL code, we have completely optimised all the structures examined; these are the four polymorphs QUA, SOD, CHA and ATN, in both AlPO and GaPO compositions. The results obtained are useful to investigate which are the important features of the Al(Ga)–O and P–O bonding in the materials, and to contrast their behaviour with that of the Si–O bonds in silica zeolites. In the analysis of the results we focus primarily on the short-range order properties, and compare bond distances, ionic charges and bond-populations in the materials examined. Our results are summarised in Table 1. All the quantities cited above show only minor variations in the different polymorphs studied, suggesting that the short-range order in the structure (which is common to all the polymorphs examined) dominates the chemical properties of the framework.

Table 1
Bond distances and Mulliken population analysis of the electronic distribution, obtained with the code CRYSTAL[a]

Material	T-site	Q (T)	Q (O)	q_b (M–O)	r (M–O)
SiO_2	Si	+2.08	−1.04	0.28	1.615
AlPO	P	+2.85	−1.26	0.27	1.514
	Al	+2.19	−1.26	0.14	1.732
GaPO	P	+2.87	−1.30	0.27	1.516
	Ga	+2.33	−1.30	0.11	1.810

[a]Only the average values for the atomic and bond properties are reported; variations in the different polymorphs examined are negligible. The symbol Q refers to net ionic charge, q_b denotes the bond population, in $|e|$; r, bond distance in Å.

3.1. Bond distances

The spread in the calculated T–O bond distances for each chemically equivalent pair of atoms (T = Al, Ga, Si, P) is less than 0.01 Å around the average value; in the AlPO structures, for instance, the optimised P–O bond lengths are 1.517 and 1.519 Å (QUA); 1.517 Å (SOD); 1.508, 1.510, 1.514 and 1.518 Å (CHA); 1.511, 1.515, 1.516 and 1.519 Å (ATN). In the following discussion, we report only the average T–O bond distance in the four polymorphs examined, and the difference of the minimum and maximum values from the average. The calculated bond lengths in the AlPO's are 1.732 ± 0.008 Å (Al–O) and 1.514 ± 0.006 Å (P–O); the corresponding values in the GaPO frameworks are 1.810 ± 0.010 Å (Ga–O) and 1.516 ± 0.006 Å (P–O). The very similar P–O bond distance in AlPO's and GaPO's validates the result that the important features of the P–O bond are due to the chemical (atomic) properties of the two atoms involved, rather than to the long-range order in the structure.

As a comparison, the equilibrium Si–O bond distance in zeolites, calculated with CRYSTAL using the basis set 6-31G(d) of reference [25], equivalent to the one employed here for AlPO's and GaPO's, is 1.615 ± 0.006 Å, intermediate between the P–O and Al–O values.

The DMOL^3 calculations on AlPO-34 (CHA), in which the cell parameters have been fixed at the experimental value of the isostructural Co-AlPO-44 [28], and after full optimisation of the internal coordinates, yield average bond distances of 1.75 Å (Al–O) and 1.54 Å (P–O); these values are overestimated by approximately 1.5% compared to the CRYSTAL results.

We have repeated the optimisation of QUA-structured AlPO (berlinite) with CRYSTAL, employing a different k-point sampling in reciprocal space, and different cut-off tolerances for the selection of integrals; neither change affected the optimised bond distances by more than 10^{-4} Å; the small difference in the calculated bond distances between the two codes employed is, therefore, a consequence of the different Hamiltonian used, HF in CRYSTAL and DFT in DMOL^3. Similar differences between bond lengths calculated at the HF and DFT levels are not surprising, and our calculated values are in sufficiently good agreement to validate both sets of calculations performed.

Experimental determinations of the bond distances can be obtained from EXAFS studies, which focus on the local structure around selected atoms. The available data for AlPO frameworks, in which Al–O is 1.73 Å and P–O is 1.51 Å [29], are in agreement with our calculations.

3.2. Electronic distribution

The electronic distribution in the structures, quantified via a Mulliken population analysis of the equilibrium electronic density obtained in the CRYSTAL calculations, is summarised in Table 1. Again, for each chemical composition, the four polymorphs examined show only marginal differences; in Table 1, we have reported the average value among all the polymorphs. The net ionic charges and the T–O bond populations, suggest that the P–O and Al(Ga)–O bonds are considerably different. While the Al(Ga)–O interaction has parameters similar to ionic materials, with the net charge of Al and Ga close to the formal value of $+3$, and a relatively small Al(Ga)–O overlap population, P and O appear to form a rather covalent bond. The net charge of P is only half the formal value of $+5$, and the P–O bond has an overlap population of 0.27 electrons, twice the value of Al–O and Ga–O bonds. The values calculated for the Si–O bond in the silica structures are similar to those of the P–O bonds, and suggest an important covalent component in the interaction.

Results of the Mulliken population analysis, in particular concerning the bond charges, are basis set dependent and affected by a degree of arbitrariness in the partition of charges; to investigate further the different properties of the Al–O and P–O bonds, we shall perform a detailed analysis based on graphical comparisons of the electronic structure. In Figs. 2 and 3, we have plotted the calculated electronic density in the AlPO-34 (CHA) structure; in particular, Fig. 2 contains the calculated electronic density in a plane intersecting a six-membered ring of the structure, as obtained with CRYSTAL; Fig. 3 shows instead a three-dimensional isodensity plot of the total electronic density calculated with DMOL^3. The latter is drawn using an isodensity value of $0.02|e|/\text{Å}^3$, and corresponds to a plot of the electronic charge due to the valence electrons.

Both pictures, combined with the results of the Mulliken population analysis discussed earlier, give unam-

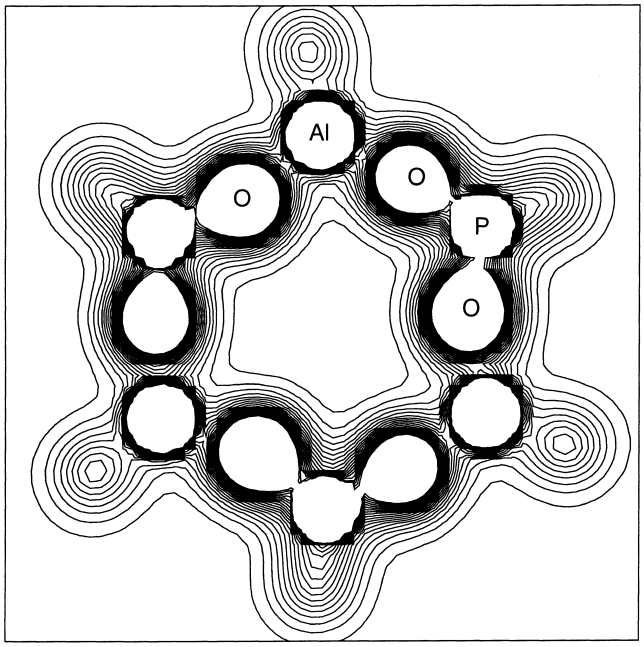

Fig. 2. Total electronic density plot in a plane intersecting a six-membered ring in AlPO-34 (CHA), as obtained with CRYSTAL. Isodensity values are plotted from 0.0 to 0.2 a.u. ($|e|$/bohr^3), with a step of 0.01 a.u.

biguous information on the nature of the AlPO framework: the Al–O and P–O bonds are such that the AlPO structure is not formed by a continuous covalent network, but rather it separates into discrete Al^{3+} and *ortho*-phosphate (PO_4^{3-}) ionic units, held together in the crystal structure by their Coulomb interaction.

To support further this unexpected finding, in Fig. 4 we show the difference electron density maps (obtained as the difference between the electron density in the solid and the superposition of isolated formal ions) and the Laplacian of the electron density ($\nabla^2\rho$) which is at the basis of the Bader's topologic analysis [30]; both quantities have been calculated with CRYSTAL, in a plane containing one Al–O–P, or the corresponding Ga–O–P and Si–O–Si units, in QUA-structured materials. As for the bond distances and Mulliken charges, very similar results were obtained for the microporous polymorphs investigated.

The information that can be derived from the difference electron density maps relates to the electronic population of the valence atomic orbitals on the T ions (Al, Ga, P and Si) compared with a perfectly ionic solution; the more electrons are associated with the T ion in this difference density, the more its bonding with the neighbouring oxygens is covalent. We clearly see in Fig. 4 that, while the difference density shows almost no feature on Al and Ga, which can, therefore, be described as ionic, an important fraction of the valence electronic density is associated with Si and even more so with P. Moreover, the electronic redistribution shows clear maxima in the direction of the Si–O and P–O bonds.

Bader's theory of 'Atoms in Molecules' [30], employs the Laplacian of the electronic density to distinguish between ionic and covalent interactions, in a way complementary to the analysis of results employed earlier in the discussion. Positive values of the Laplacian are associated with zones of ionic interactions in the structure; negative values are instead associated with zones of electronic build-up within covalent bonds. In Fig. 4, we see that in AlPO's and GaPO's there is an ample zone of negative Laplacian along the P–O bonds; again the P–O interaction appears covalent, although polarised towards the oxygen atoms (the zone of negative Laplacian is centred on the oxygen). The Al–O and Ga–O bonds have, in-

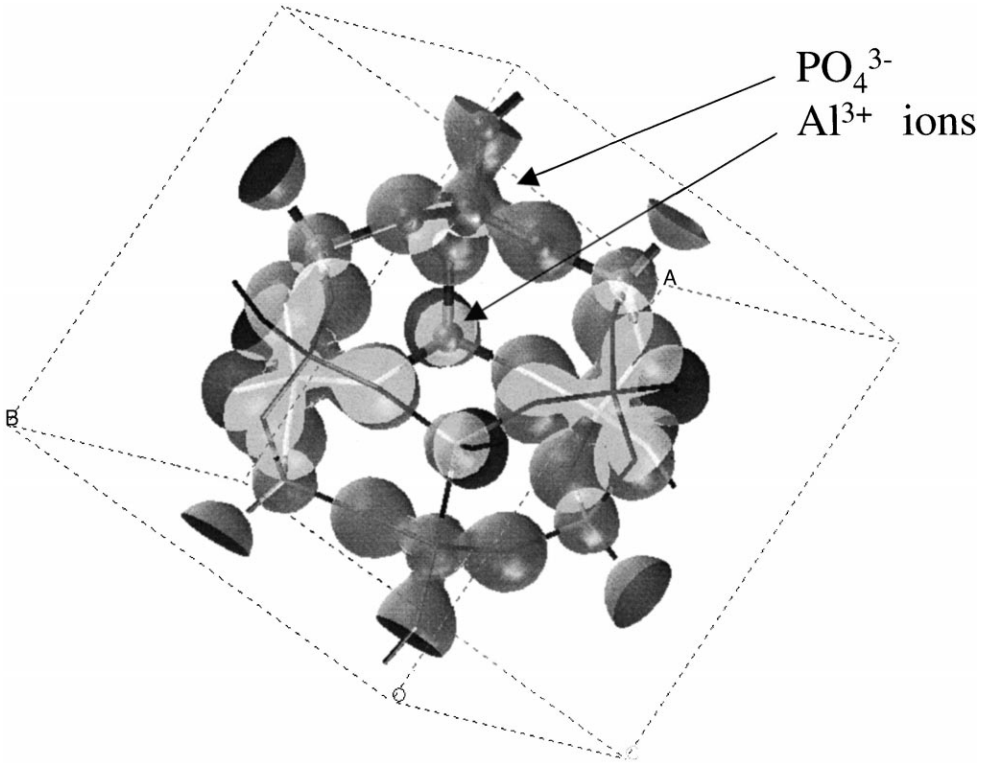

Fig. 3. Three-dimensional isodensity plot ($\rho = 0.02|e|/\text{Å}^3$) of the electronic density in the unit cell of AlPO-34 (CHA), calculated with DMOL[3]. Note the natural separation of the structure into discrete Al^{3+} and PO_4^{3-} ions.

stead, a positive Laplacian, which only displays a minor polarisation of the electronic shell on the oxygen towards the Al (Ga) species. The Si–O bond in zeolites has intermediate behaviour between the Al–O and P–O bonds, but still causes an appreciable distortion of the electronic density around the oxygens. A small area with a negative Laplacian is also present along the Si–O directions.

As a conclusion from all the above arguments, we deduce that the Si–O bonds in zeolites and the P–O bonds in AlPO's and GaPO's have large degrees of covalence, while the Al–O and Ga–O bonds are ionic.

Obviously, such a result has important consequences for our understanding of AlPO and GaPO materials. The ionicity of the AlPO framework can effectively explain several pieces of experimental information on AlPO's, and hence provide an indirect validation of the modelling results: AlPO's, for instance, show a much less pronounced resistance than zeolites when steamed. While the covalent Si–O backbone is resistant to the treatment, the ionic backbone of AlPO's dissolves. The framework ionicity also suggests that defects with ionic character are more likely to occur in the 3+ sites of the AlPO and GaPO materials than in SiO_2 zeolites. Late transition metal cations, such as Ni, Mn, Co or Fe, have a bonding with the oxygens with a similar degree of ionicity to the Al–O in AlPO's obtained here (which is due to the contracted size of their valence d-AO's [31,32]), which may explain why such cations can be more easily substituted in the AlPO framework than in zeolites. Furthermore, we consider that it is the strong field created by the four PO_4^{3-} nearest neighbours which is able to constrain the Co^{3+} ions into the unusual tetrahedral coordination.

From a theoretical chemistry point of view, the separation of the AlPO framework into ionic Al^{3+} and PO_4^{3-} units has also important consequences. If we

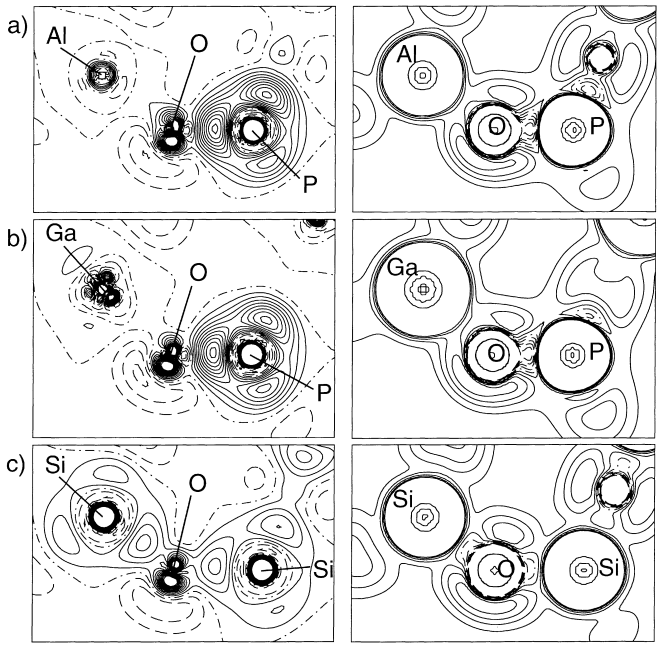

Fig. 4. Difference electron density maps (solid minus isolated formal ions) (left plots), and Laplacian of the electron density (right plot) in a plane containing one Al–O–P unit in quartz-structured AlPO (a), Ga–O–P unit in GaPO (b) and Si–O–Si unit in SiO_2 (c). Continuous, dashed and dot–dashed lines correspond to positive, negative and zero values of the function plotted.

had to employ simplified cluster models to represent the solid, a saturation of the terminal atoms with hydrogens as employed for silica zeolites, would impose a degree of covalence to the terminal OH bonds that does not correspond to the results expressed earlier. In this case, it would seem more appropriate to exploit the natural separation of the framework into discrete ions, and employ a molecular fragment composed of an integer number of Al^{3+} and PO_4^{3-} units, together with an embedding potential which reproduces the Coulomb field generated by the rest of the infinite framework.

3.3. Framework stability

The calculated energies can be employed to derive a relative order of stability of the structures examined; a summary of results is reported in Table 2.

For both AlPO and GaPO materials, we find E(QUA)<E(SOD)<E(ATN)<E(CHA); the order of stability of QUA, SOD and CHA polymorphs is the same as obtained in [25] for zeolites. This parallel behaviour indicates that the long-range order in the structure plays a similar rôle in isostructural materials with different chemical composition. The chemical composition of the framework, however, still influences its relative stability: the energy difference in AlPO's is greater than that calculated in zeolites, and the values become even larger for the GaPO frameworks. The latter comparison suggests, therefore, greater difficulty in synthesising AlPO's and especially GaPO's microporous frameworks compared to zeolites. We propose the following explanation: the net charge on the oxygens is larger in AlPO's and

Table 2
Relative stability of the polymorphs examined, as obtained from the CRYSTAL calculations[a]

Material	QUA	SOD	ATN	CHA
SiO_2[25]	0.0000	+4.6	–	+6.3
AlPO	0.0000	+11.8	+12.2	+13.9
GaPO	0.0000	+14.6	+21.5	+34.9

[a]Results are reported in kJ/mole of TO_2 units; the energy values for the silica polymorphs are obtained from [25], using the 6-31G(d) basis set and the HF Hamiltonian, which correspond to our calculations on AlPO's and GaPO's.

GaPO's than in zeolites (see Table 1); on average, the framework structure is, therefore, more ionic in the former materials. The higher ionicity, especially concerning the bonding of the 3+ ions, increases the importance of the Madelung field in determining the relative structural stability, and hence increases the energy toll to pay when the density of the crystal decreases from the dense to the microporous polymorphs. This feature explains the higher energy difference between isostructural polymorphs in AlPO's and GaPO's compared to zeolites. A similar effect, but of even greater magnitude, was found in reference [6,7] on examining the molybdenum and tungsten trioxides.

Both our findings, the ionicity of the AlPO framework and the higher energy of the microporous polymorphs relative to the stable QUA structure compared to zeolites, are consistent with experiment, in that microporous AlPO structures collapse more easily than their isostructural zeolites.

4. The Co substitution in AlPO (CHA)

After the description of results concerning the pure, undoped framework of microporous aluminium and gallium phosphates, we now examine the chemistry that follows the doping of such structures with late transition metal ions. We focus in particular on the Co-AlPO-44 system, obtained by including substitutional Co^{II} or Co^{III} ions in the framework of AlPO-34 (CHA), as this material is the object of experimental studies in our laboratory.

All the calculations that we describe in this section have been performed using DMOL[3], with either one or two Co ions in each unit cell of the Co-AlPO-44 (CHA) structure (which contains six $AlPO_4$ formula units, i.e. 36 ions). This level of Co doping is much higher than achievable experimentally, but the complexity of the calculations is such that the 36-ion periodic unit, in the absence of symmetry elements that can reduce the computational burden, is the biggest affordable routinely. Even with this unit cell, each calculation performed has required the optimisation of $(36 \times 3) = 108$ independent degrees of freedom in the periodic system.

The electronic distribution of the Co ions, in both oxidation states +2 and +3, has been imposed in our calculations to be of high-spin; $d^{(6)}$ with spin 2 for Co^{III}, and d^7 with spin 3/2 for Co^{II}. Furthermore, only 'ferromagnetic' structures have been examined, in which the spin of all the Co ions is aligned. Even in the highest doping concentrations examined, the two nearest Co ions are separated by at least four bonds in the structure; we consider that in such a case, the spin interaction among Co ions can be considered as negligible.

The aim of our calculations was to understand the acid and redox properties of substitutional Co ions in the AlPO framework. We have, therefore, simulated several defect structures, which represent isolated and pairs of substitutional Co^{III} ions in the framework; their reduction with H_2, yielding Co^{II} ions and Brønsted acid sites has also been examined. Furthermore, we considered the possible involvement of framework oxygens next to the substitutional Co ions in redox reactions, by creating a defect cluster containing two Co^{II} ions and one neighbouring oxygen vacancy. The latter situation is depicted schematically in Fig. 5.

We have optimised the geometry, and calculated the electronic density and energy, of each of the above defect centres. Fig. 6 gives a comprehensive picture of the chemistry examined, and of the energy change

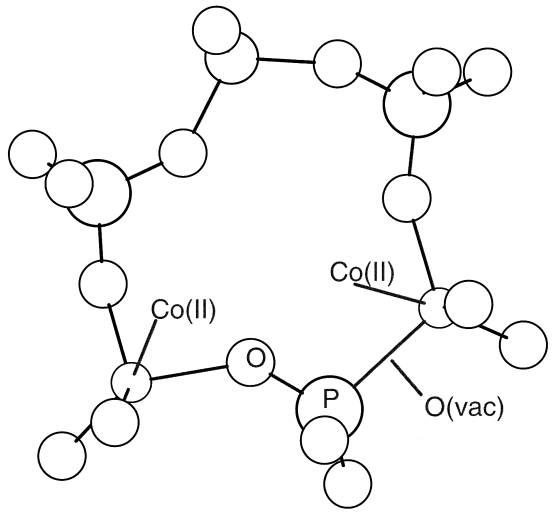

Fig. 5. Schematic representation of a Co-containing defect centre in AlPO's. The case shown contains two substitutional Co^{II} ions in a six-membered ring of the CHA structure, charge-compensated by a framework oxygen vacancy.

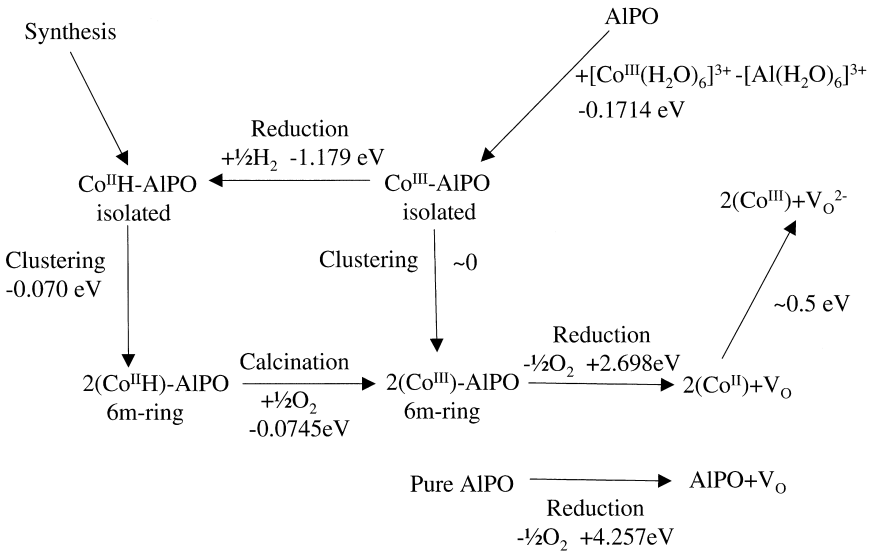

Fig. 6. Energetic balance of several redox reactions involving substitutional Co ions in Co-AlPO-44, as obtained via periodic DFT calculations using the code DMOL[3].

in each step. We now describe the most important findings of our work, and where possible we compare our results with available experimental evidence.

1. The replacement energy ΔE of a framework Al with a Co^{III} ion, according to the reaction

$$Al_{framework} + [Co(H_2O)_6]^{3+} \rightarrow Co^{III}_{framework} + [Al(H_2O)_6]^{3+} \quad (1)$$

is calculated as -0.1714 eV (16.53 kJ/mol) for an isolated Co^{III} centre, indicating the possibility of including Co^{III} ions into the AlPO framework during the synthesis.

The four Co^{III}–O distances are calculated, in order of increasing bond length, as 1.852, 1.867, 1.880 and 1.896 Å, considerably larger than the original Al–O bond distances in the host framework. Experimental EXAFS studies [14] indicate a non-uniformity of the Co^{III}–O bond lengths, which has been rationalised in terms of three short and one longer bond distances, of 1.83 and 2.04 Å. Our results suggest a more uniform spread of Co^{III}–O bond distances, at least in the long-range ordered material simulated with our calculations; the average Co^{III}–O bond lengths from experimental and theoretical works are however in good agreement.

2. When two Co^{III} ions are substituted in the same four-or six-membered ring of the host material, the replacement energy is little changed to -0.1664 eV (16.05 kJ/mol) per Co ion. The calculations indicate, therefore, that no energy barrier opposes the clustering of Co ions, and that the distribution of Co in Co-AlPO-44 can be assumed as *statistical*; it is probably dictated by the Coulomb interactions with the cationic templates during the synthesis. At high Co loadings, two or more Co sites are likely to be present in near neighbour sites.
3. Redox reactions have been investigated by reducing the framework Co^{III} dopants with H_2, yielding Co^{II} and a Brønsted acid site on one of the oxygens nearest neighbour of Co^{II}. The reaction is energetically favourable, with a calculated ΔE of -1.179 eV (113.75 kJ/mol) for the isolated Co^{III} centre. The stability of substitutional Co as Co^{II} in the AlPO framework is in agreement with the experimental evidence; after the synthesis, CoAlPO materials generally have a deep blue colour due to the Co^{II} ions. Co in oxidation state $+3$ is only obtained upon calcination with O_2 (see [14]).

The calculated bond distances involving Co^{II} ions are 1.925, 1.939, 1.941 and 2.134 Å; the latter is relative to the Co^{II}–O(H) bond with the Brønsted

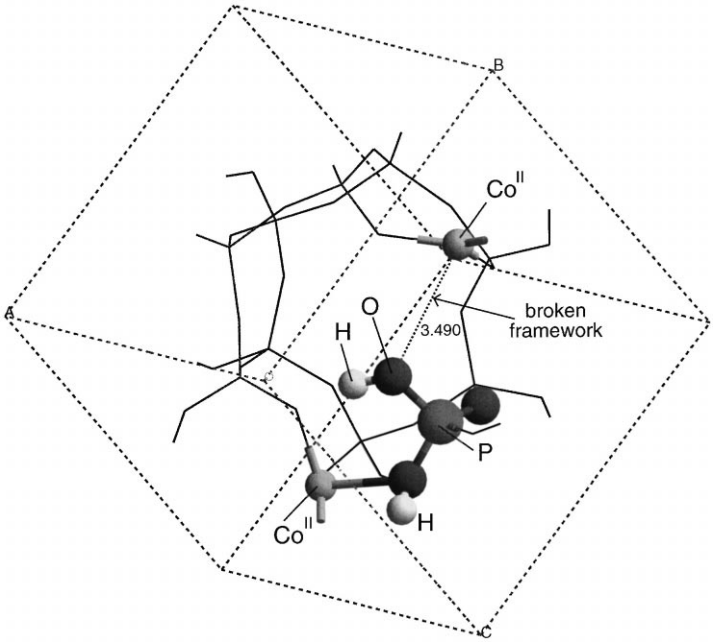

Fig. 7. Equilibrium geometry of the defect centre containing two substitutional Co^{II} ions in a six-membered ring of Co-AlPO-44, charge-compensated by two Brønsted acid protons. H-bonding interactions between the H-bond donor OH group and the rest of the framework are sufficient to break the framework connectivity.

acid site. EXAFS studies provide a value of 1.90 Å for the three shorter Co^{II}–O bonds, and of 2.04 Å for the Co^{II}–O(H) [14].

4. In the case in which two Co^{III} occupy the same six-membered ring, reduction via H_2 becomes energetically more favourable compared to the isolated Co^{III} ions, with an extra stabilisation energy of 0.070 eV (6.75 kJ/mol) per pair of Co ions. Full relaxation of the framework shows that the extra stabilisation is due to H-bonding interactions between the two acid OH groups created upon reduction and the other oxygens of the AlPO framework. The strength of the H-bond is sufficient to break the framework connectivity at the H-bond donor OH group; the distance of the O in the latter group from the nearest Co^{II} ion increases to 3.49 Å. A picture of the equilibrium configuration is shown in Fig. 7. We consider that the framework *opening* under the effect of an H-bond confirms once more the ionicity of the AlPO structure. The PO_4^{3-} unit sandwiched between the two substitutional Co^{II} ions behaves in such a case as an $H_2PO_4^-$ ion, whose Coulomb interaction with the neighbouring cations (the two substitutional Co^{II} and the two Al^{3+} at the regular lattice sites) is greatly reduced. Even an H-bond, which we would consider energetically less important than the O–Co^{II} interaction, is in this case of sufficient strength to distort the local structure, to such an extent that the framework connectivity is effectively broken. The latter result suggests that the CoAlPO framework is indeed structurally unstable at high Co loadings, in agreement with experiment.
5. Calcination of two Co^{II} sites with O_2, yielding two Co^{III} and water, is energetically favourable for the Co-AlPO-44 structure; its calculated ΔE is -0.0745 eV (7.19 kJ/mol), again in agreement qualitatively with experiment, which shows that in Co-AlPO-44 after calcination, more than 90% of Co is present as Co^{III}.
6. Reduction of Co^{III} via the desorption of a framework O atom is energetically unfavourable ($\Delta E = +2.698$ eV, 260.3 kJ/mol), but the presence of Co^{III} activates the framework oxygen towards desorp-

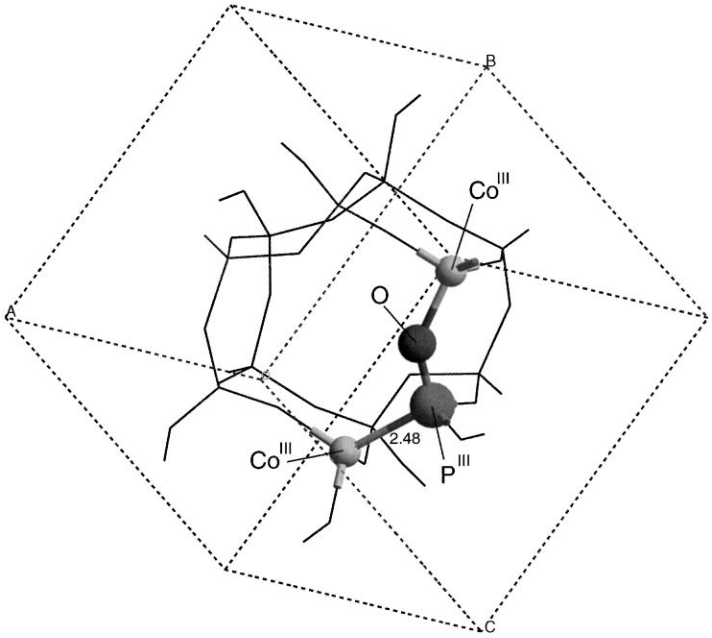

Fig. 8. Equilibrium geometry of the defect centre formed upon creation of a framework O vacancy, and containing two Co^{III} and a reduced P^{III} ions.

tion; the same reaction in the pure AlPO framework has a calculated ΔE of +4.257 eV (410.7 kJ/mol). The participation of framework oxygens in the catalytic cycle is not unlikely, especially when high-temperature or high-energy treatments of the CoAlPO catalyst are involved at some stage during either its synthesis or the catalytic reaction itself.

7. Finally, it is worth mentioning that in the reaction leading from two Co^{III} to two Co^{II} via the formation of a framework oxygen vacancy, the system has converged to two different electronic configurations, separated by an energy barrier of less than 0.5 eV. In the stable electronic state, the two electrons left by the desorption of atomic oxygen are ceded to the Co-d atomic orbitals; the two extra electrons, therefore, reduce the two substitutional Co^{III} to Co^{II}. The second electronic state is more similar to an F centre in ionic solids: the Co^{III} ions are in this case unchanged, and the two extra electrons populate the atomic orbital on P left empty on the desorption of oxygen. In this case it is, therefore, the P atom that is reduced, from oxidation state +5 to oxidation state +3. During the geometry optimisation, the Co^{III}–P^{III} distance across the oxygen vacancy decreases to 2.48 Å (see Fig. 8). It is possible that the coordination number lower than four estimated for the Co^{III} ions from the EXAFS study may be due to the latter electronic defect, or to similar configurations of the material.

5. Conclusions

We have presented an extensive treatment of microporous AlPO and GaPO molecular sieves, and of their defect chemistry obtained upon doping with Co.

In contrast with the properties of the silica forms (zeolites), the tetrahedral backbone of AlPO's and GaPO's is not formed by a continuous network of covalent T–O bonds, but rather by discrete Al^{3+} (or Ga^{3+}) and PO_4^{3-} ionic units. Much of the chemistry of AlPO's relates to this ionic character, from the instability upon steaming, to the possibility of incorporating dopant ions which themselves give ionic bonding with the oxygens, such as Co.

Even weak interactions, such as an H-bond involving the Brønsted acid OH group, created to charge-compensate the framework Co^{II} substitutions, may have sufficient strength to break the AlPO framework in its weakest point, i.e. the ionic $Co^{II} \cdots O(H)$–P bond.

Acknowledgements

Useful discussions have taken place during the course of this work with several researchers and visitors of the Royal Institution. We are particularly indebted to Prof. Sir J.M. Thomas, Dr. G. Sankar, Dr. A. Sokol and Dr. R. Alvarez for their valuable contribution.

Molecular Simulations Inc. is thanked for providing the latest version of the code $DMOL^3$, which has been determinant for the examination of the Co-AlPO material. EPSRC is gratefully acknowledged for funding this research project and for the provision of time on the IBM/SP2 computer at the Daresbury Laboratory, where the CRYSTAL calculations have been performed.

References

[1] J.M. Thomas, Sci. Am. 267 (1992) 12.
[2] M.M.J. Treacy, B.K. Marcus, M.E. Bisher, J.B. Higgins (Eds.), Proceedings of the 12th International Zeolite Conference, Materials Research Society, Warrendale, 1999.
[3] Y.F. Shen, S.L. Suib, C.L. Oyoung, J. Am. Chem. Soc. 116 (1994) 11020.
[4] Y.F. Shen, R.N. Deguzman, R.P. Zerger, S.L. Suib, C.L. Oyoung, Stud. Surf. Sci. Catal. 83 (1994) 19.
[5] S.R. Wasserman, K.A. Carrado, S.E. Yuchs, Y.F. Shen, H. Cao, S.L. Suib, Physica B 209 (1995) 674.
[6] F. Corà, D.W. Lewis, C.R.A. Catlow, Chem. Commun. 1998, 1943.
[7] F. Corà, C.R.A. Catlow, D.W. Lewis, J. Mol. Catal., this issue.
[8] M. Taramasso, G. Perego, B. Notari, US Patent 4410501 (1983).
[9] G. Perego, G. Bellussi, C. Corno, M. Taramasso, F. Buonomo, A. Esposito, Stud. Surf. Sci. Catal. 28 (1986) 129.
[10] P.A. Barrett, G. Sankar, C.R.A. Catlow, J.M. Thomas, J. Phys. Chem. Solids 56 (1995) 1395.
[11] G. Sankar, J.K. Wyles, R.H. Jones, J.M. Thomas, C.R.A. Catlow, D.W. Lewis, W. Clegg, S.J. Coles, S.J. Teat, Chem. Commun. (1998) 117.
[12] J.M. Thomas, R. Raja, G. Sankar, R.G. Bell, Nature 398 (1999) 227.
[13] G. Sankar, R. Raja, J.M. Thomas, Catal. Lett. 55 (1998) 15.
[14] P.A. Barrett, G. Sankar, C.R.A. Catlow, J.M. Thomas, J. Phys. Chem. 100 (1996) 8977.
[15] J. Sauer, in: C.R.A. Catlow (Ed.), Modelling of Structure and Reactivity in Zeolites, Academic Press, San Diego, 1992, p. 183.
[16] P.E. Sinclair, C.R.A. Catlow, J. Phys. Chem. 103 (1999) 1084.
[17] P.E. Sinclair, A. DeVries, P. Sherwood, C.R.A. Catlow, R.A. VanSanten, J. Chem. Soc., Faraday Trans. 94 (1998) 3401.
[18] M. Sierka, J. Sauer, Faraday Dis. 106 (1998) 41.
[19] P. Sherwood, A.H. de Vries, S.J. Collins, S.P. Greatbanks, N.A. Burton, M.A. Vincent, I.H. Hiller, Faraday Dis. 106 (1998) 79.
[20] C. Pisani, R. Dovesi, C. Roetti, Hartree-Fock Ab Initio Treatment of Crystalline Systems, Lecture Notes in Chemistry, Vol. 48, Springer, Heidelberg, 1988.
[21] V.R. Saunders, R. Dovesi, C. Roetti, M.Causà, N.M. Harrison, R. Orlando, C.M. Zicovich-Wilson, CRYSTAL 98 User's manual, University of Torino, Turin, Italy, 1998.
[22] $DMol^3$ User Guide, September 1997, Molecular Simulations Inc., San Diego, 1997.
[23] B. Delley, J. Chem. Phys. 92 (1990) 508.
[24] J.P. Perdew, Y. Wang, Phys. Rev. B 45 (1992) 13244.
[25] B. Civalleri, C.M. Zicovich-Wilson, P. Ugliengo, V.R. Saunders, R. Dovesi, Chem. Phys. Lett. 292 (1998) 384.
[26] M. Catti, G. Valerio, R. Dovesi, M. Causà, Phys. Rev. B 49 (1994) 14179.
[27] R. Pandey, J.E. Jaffe, N.M. Harrison, J. Phys. Chem. Solids 55 (1994) 1357.
[28] G. Muncaster, G. Sankar, C.R.A. Catlow, J.M. Thomas, R.G. Bell, P.A. Wright, S. Coles, S.J. Teat, W. Clegg, W. Reeve, Chem. Mater. 11 (1999) 158.
[29] G. Sankar, private communication.
[30] R.F. Bader, Atoms in Molecules: A Quantum Theory, International Series of Monographs on Chemistry, Vol. 22, Clarendon Press, Oxford, 1990.
[31] P.A. Cox, Transition Metal Oxides, an Introduction to their Electronic Structure and Properties, International Series of Monographs on Chemistry, Vol. 27, Clarendon Press, Oxford, 1995.
[32] M.D. Towler, N.L. Allan, N.M. Harrison, V.R. Saunders, W.C. Mackrodt, E. Aprà, Phys. Rev. B 50 (1994) 5041.